

Numerical modelling of tracer tests in the Ohaaki geothermal system

Marloes van Driel^{1,2}, Theo Renaud¹, Michael Gravatt¹, Michael O'Sullivan¹, John O'Sullivan¹, Jeremy Riffault¹, Adrian Croucher¹, F. N. van de Vosse², Nataly Castillo Ruiz³

¹Geothermal Institute, University of Auckland, 70 Symonds Street, Grafton, Auckland, 1010, New Zealand

²Eindhoven University of Technology, Eindhoven, The Netherlands

³Contact Energy Limited, Wairakei, New Zealand

theo.renaud@auckland.ac.nz

Keywords: *Waiwera, Ohaaki, Tracer tests.*

ABSTRACT

The Ohaaki geothermal field (OGF) is a gassy two-phase geothermal field in the volcanic and sedimentary accumulation basin at the eastern margin of the Taupo Volcanic Zone in the central North Island of New Zealand.

The long history of exploration and development of Ohaaki started with the drilling of the first well in 1965. Large-scale testing of the production wells was conducted from 1965 to mid-1971, and power production commenced in 1989.

Many tracer tests have been carried out at Ohaaki to better understand flow pathways between wells. The aim of the present study is to use modelling of these tracer tests to help in improving the calibration of a reservoir model.

First the available information about the historical tracer tests in Ohaaki was collected and reviewed. Three of the tracer tests were selected as the first group to be used for modelling using the parallel open-source simulator Waiwera and the latest Ohaaki model developed at the University of Auckland.

Good agreement is shown between the data and the model results for some wells. For other wells where agreement is not satisfactory the mismatch is used to decide on improvements that should be made to the permeability structure of the model.

1. INTRODUCTION

1.1 Ohaaki Tracers Tests

Between 1974 and 2018 a total of 41 tracer tests were carried out in the OGF. To select tests suitable for simulation a review of the tracer tests was conducted, and three tests were selected for simulation. Two criteria were used in selecting these tests: first, there had to be a good response measured in at least one well and second, the tests were spread around the field and over time.

To run a simulation of a tracer test, the following data must be available:

- The well in which the tracer was added,
- The xyz location of the feedzones in the injection well,
- The tracer that was added,
- The amount of added tracer,
- The period over which the tracer was added,
- The mass flow at the injection well,
- The wells which were monitored and their mass flows,

- The xyz location of the feedzones in the monitor wells,
- The response at the monitor wells (preferably mass fraction of tracer vs time).

Preferably data and graphs showing the amount of response should also be available.

Ideally, accurate daily historical production and reinjection data should also be available, but often these data were not measured during the tracer tests.

Well-by-well production and injection rates are not continuously measured at Ohaaki and for our reservoir model we calculate them from values measured for groups of wells, e.g., those production wells feeding a particular separator, and from the fraction for a particular well of the combined flow determined by annual performance tests. We then assume that the well-by-well fractions of the combined flow stays constant over the next year. However, these fractions are modified for periods when it is known that a particular well is taken offline.

For some of the tracer tests, flow rates of the affected wells were measured during the test and in these cases more accurate well-by-well production and injection rates were included.

1.3 Tracer test selection

The early tracer tests carried out at Ohaaki by the Institute of Nuclear Sciences were summarized by Bullivant et al. (1990) (14 tests) and Grant (2011) (34 tests). Grant's compilation was based on an unpublished list in the records of Contact Energy Limited, the compilation of Bullivant et al. (1990) and a sequence of reports by McCabe (McCabe, 1990, 1991, 1992a,b, 1993, 1994, 1995a,b,c; McCabe et al., 1994).

Three tests were selected for the first group of simulations with the reservoir model: Test 3, Test 13 and Test 29 (we numbered the tests in chronological order). As mentioned above, the main criterion for selection was whether there were some reasonable responses in some of the monitor wells. Otherwise, a spread in time and space was sought. Details of the three tests are given in the Appendix.

Test 3. Test 3 is an early test for which there was a good response at the two monitor wells. On 21st May 1977, 270 GBq of ¹³¹I was added to the water from a cooling pond, containing separated geothermal water from BR11, which was being reinjected into BR33 while BR8 and BR11 were monitored (McCabe et al., 1983). A mass of separate geothermal water of 210 t/h was injected into BR33 from 20-02-1977 to 20-09-1977 (Clotworthy, 1989).

Test 13. In Test 13 the precise daily injection rate for the tracer injection well, BR20, is known until 64 days after the test. On 17-10-1985, 780 GBq of ^{131}I was injected into BR20. BR13, BR19 and BR22 were monitored (Bullivant et al., 1990). The discharge history of well BR13 was also given in Bullivant et al. (1990) and this was added to a file (BR13 data.json) used to set up the production data for BR13 in the reservoir model.

Test 29. For this test, on 06-06-1991, 19.38 GBq of ^{125}I was injected into well BR7. The injection mass flow in BR7 was 220 t/hr over a period of 170 days. Wells BR10, 13, 14, 24, 25, 27, 29, 35, 36, 42, 43, 44, 45 were monitored (McCabe, 1992; McCabe et al., 1995). In the file (BR7 data.json) used in our modelling framework (O’Sullivan et al. 2023a) to set up the production/injection data, provided by Contact Energy Limited, for BR7 in the reservoir model there was already weekly mass injection rates of about 50-70 t/hr during the test period. It was assumed that data from the tracer test report was more accurate, and so the file was altered.

The radioactive iodine tracers were usually added by breaking a flask lowered into the injection well and thus would have been added almost instantaneously. Bixley (private communication) suggested that the other tracers would have been added over a period of less than 30 minutes. For modelling, times of 20 seconds and 15 minutes respectively, were used.

2. NUMERICAL MODEL

2.1 Background

The geothermal modelling group at the University of Auckland (UoA) has been carrying out numerical modelling of the Ohaaki system for Contact Energy Limited (CEL) and its predecessors since the 1980s. There have been many versions as the model evolved to incorporate new measured data and to exploit new computational tools.

For the modelling report presented in 2013, as part of the application for renewal of resource consents, a model with 22816 computational blocks was used (Model OH22816). After the hearing it was decided that more details in the shallow zone were required and several more, thinner, layers were added giving a model with 43102 blocks (Model OH43102).

Model OH22816 and Model OH43102 both had the top surface set at the estimated elevation of the water table. In 2014 it was decided to set the top of the model at ground surface so that the model could include the vadose zone and could track changes in the groundwater level. The same model grid in plan-view was used but because of the extension of the model to ground surface more model blocks were used, creating Model OH45250.

Late in 2015 it was decided more resolution in the production area was required and a model with mesh refinement was set up with 35446 model blocks (Model OH35446). The previous models all used a “tartan” grid with small mesh size in the production area but no specific mesh refinement and therefore Model OH35446 gave more mesh refinement in the production area but contained overall fewer blocks.

Also, in 2015 it was decided, that because some of the recent deep wells extended quite close to the base of the model, it should be deepened. An extra 4 layers (1 km) were added creating model OH38582.

In 2022 we introduced a new model grid (see Figure 1) and created model OH68954. The main aim with this model was to better match some features of the conceptual model, namely, the faults and the clay cap (alteration zone), while also improving upon the already good state of calibration achieved with models OH35446 and OH38582.

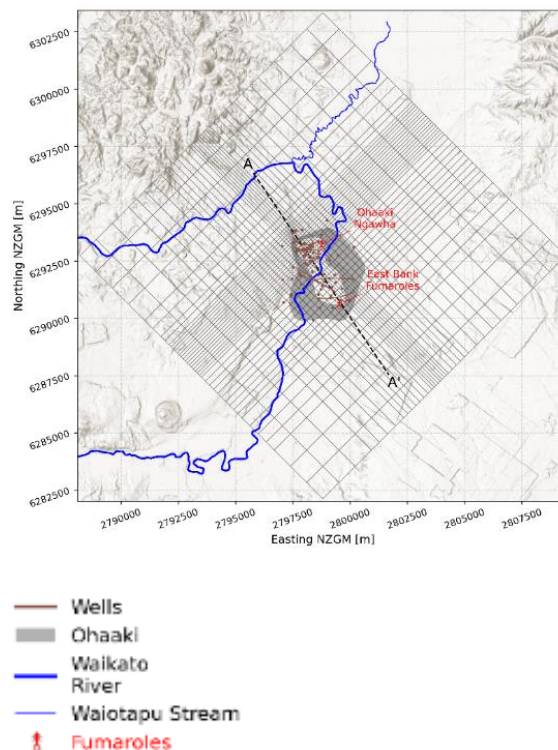


Figure 1: Model grid for Model 68954, showing the river and resistivity boundary (slice AA' is used in some plots below).

A second aim was to set up a model that could be run using either AUTOUGH2 (Yeh et al., 2012) or the highly parallelized simulator Waiwera (Croucher et al., 2020) and to be able to run a dual-porosity version of the model. The type of mesh refinement, with 5-sided blocks, used in Model OH35446 is not available with Waiwera and therefore for model OH68954 we reverted to a tartan grid (see Figure 1).

A final aim was to transition to the standardised modelling framework we have been developing over several years (Popineau et al. 2018; Renaud et al. 2021; O’Sullivan et al., 2023a). This framework is based on coupling a digital conceptual model from Leapfrog Geothermal software into an AUTOUGH2 (or Waiwera) computer model and then managing the model with a standardised set of transferable and transparent tools.

2.2 Conceptual Model

The conceptual model of the reservoir has improved over the years thanks to the integration of more information such as magneto-telluric data (MT) and deeper drilling data.

Recent reservoir engineering data has affected the conceptual model. For example, the West Bank deep reservoir zone has shown a large pressure decline with some pressure recovery between 2001 and 2010.

The deep reservoir is thought to be connected to the intermediate reservoir, but the pressure data suggest that there is a low permeability zone between the deep wells and intermediate level wells.

The East Bank pressure appears to be slightly higher than that in the West Bank, suggesting the existence of a separate deep upflow in the West (Mroczek et al., 2016).

Figure 2 shows a cross section from a three dimensional (3D) conceptual model discussed by Mroczek et al. (2016). The geothermal system appears to overlay the greywacke basement rocks which dip to the northwest with a horst structure in the south-east.

The Rangitaiki ignimbrite which erupted 350,000 years ago is a marker for the Whakamaru group. The Huka Falls group represent impermeable fine-grained sediments and the Waiora and Rautawiri formations are shallow tuffs. A thick Ohaaki rhyolite dome is located on the West Bank. This dome is highly faulted and permeable, allowing the geothermal fluid to rise through it.

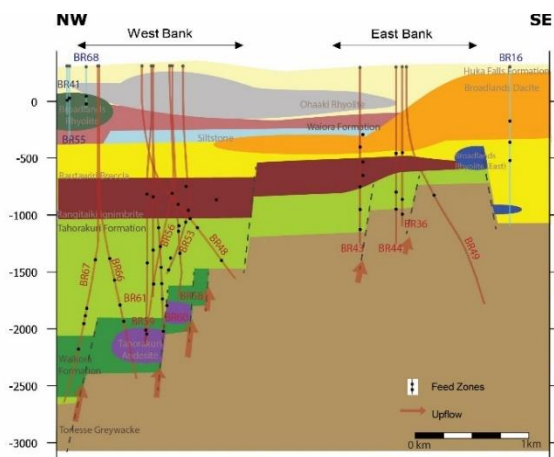


Figure 2: Cross section from a three dimensional (3D) conceptual model discussed by Mroczek et al. (2016).

2.3 Updated geological model

An updated version of the geological model has been built using Leapfrog Geothermal by GNS Science, notably mapping twelve faults in the area. Figure 3 shows the fault network, including the three regional faults, Aratiatia, Reporoa Caldera, Kaingaroa, as well as nine northeast striking faults.



Figure 3: Plan view of updated fault network shown at -2800 masl (metres above sea level) in the model. This is taken from the Leapfrog digital conceptual model.

Some faults dip to the South or North by a few degrees and thus there are small differences in the plots at different elevations. Several intersections between faults are located within the West Bank.

2.4 The clay cap

The explicit inclusion of an alteration model in the digital conceptual model allows more heterogeneity in the permeability structures of the numerical model, and this should allow a better match to the shallow temperatures. The alteration zone is represented by new rock-types in the numerical model. The inferred alteration zone, shown in Figure , has been determined from a range of data sources including MT, downhole temperature data (contoured into surfaces in Leapfrog Geothermal®), the DC resistivity boundaries, methylene blue tests on samples, and feed zone information for the wells.

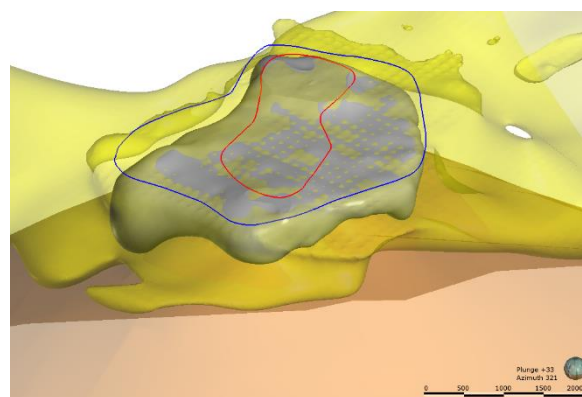


Figure 4: Clay cap (grey) showing the 9 ohm-m MT contour (yellow), the DC resistivity boundary (blue and red) and the 200°C temperature contour (orange).

2.5 Model calibration

Based on the updated digital conceptual model, the new reservoir model OH68954 (versions for AUTOUGH2 and Waiwera) was set up and calibrated. Details of the model set-

up and calibration are given in O'Sullivan et al. (2023b). Good matches to the natural state data and the production history data were obtained.

The vertical permeability on slice AA' in the calibrated model is shown in Figure 5.

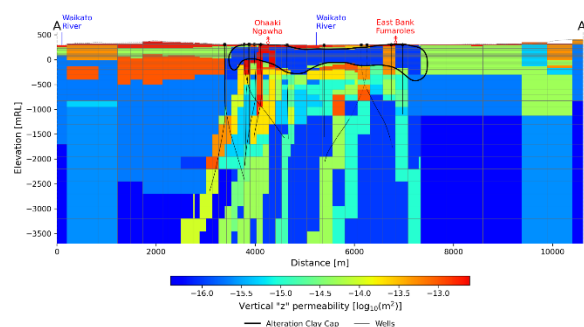


Figure 5: Vertical permeability in the NW-SE slice A-A' for Model OH68954_486.

For the production history simulations, two versions of the model were used, i.e., single porosity (SP) and dual porosity (DP, also known as MINC). DP models split each model block into multiple subdomains with different properties, denoted as fracture and matrix subdomains. The fracture subdomain has a higher porosity and permeability which typically allows transient processes to occur more quickly. Hence, a DP model is expected to be able to better represent the early boiling that occurred at Ohaaki and a DP model is expected to better match tracer test data (e.g., Gomez-Diaz, 2022)

2.6 Tracer modelling

After comparing the results of the DP model to the results of the SP model for tracer test simulations, a DP version of the model was used for all subsequent simulations. For each of the three tracer tests selected, the standard production history model was run up to a time just before the start of the test (with no tracer included). Then a tracer simulation was carried out using a tracer-capable version of Waiwera (see Croucher et al., 2021). The model file for the tracer simulations included several modifications:

- Smaller time steps were used than in the standard production history model,
- A higher resolution representation in time of the injection/production records for the wells involved in the tracer tests,
- A tracer input was included as a separate entry in the GENER module for AUTOUGH2 and its equivalent in Waiwera.

The simulation of the tracer test was run for long enough so that by the end of the simulation no significant changes in the tracer concentrations were occurring. The final conditions at the end of the first stage production history run were used as initial conditions for the tracer test simulation.

3. RESULTS

3.1 Tracer Test 3

Results for the tracer concentrations at the two monitor wells in Tracer Test 3 (BR8 and BR11) are shown in Figure 6.

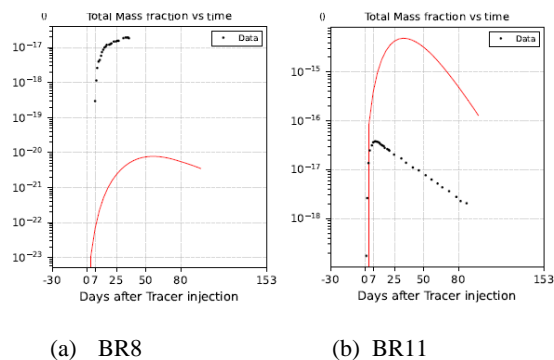


Figure 6. Results for Tracer Test 3. Mass fraction of tracer in the monitor wells BR8 and BR11 (log scale). Red lines show model results, black dots are data.

Clearly the small-scale permeability distribution in this part of the model is incorrect. The data for BR8 shows a moderate response whereas the model shows a small response. By contrast the model shows a large response at BR11 whereas the data shows a moderate response.

3.2 Tracer Test 13

Results for the tracer concentrations at the three monitor wells in Tracer Test 13 (BR13, BR23 and BR22) are shown in Figure 7.

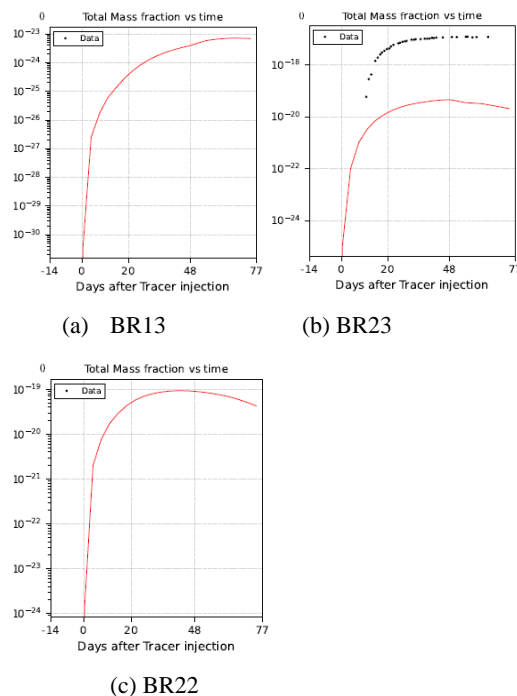


Figure 7. Results for Tracer Test 13. Mass fraction of tracer in the monitor wells BR13, BR23 and BR22. Red lines show model results, black dots are data (no response was measured for BR13 and BR22).

Again, some of the small-scale permeability distribution in this part of the model is incorrect. The model response for BR13 is small and the data shows no response. For BR23 the trend of the model response matches the data quite well. The model shows a moderate response in BR22, but the data show no response.

3.3 Tracer Test 29

Results for the tracer concentrations at twelve monitor wells in Tracer Test 29 are shown in Figure 8 and are summarized in Table 1.

Table 1: Summary of results for Tracer Test 29.

Wells	Results
BR45, BR35, BR42, BR10, BR27	Model too high
BR36, BR29	Model reasonable
BR25, BR24, BR43, BR44, BR13	Model too low

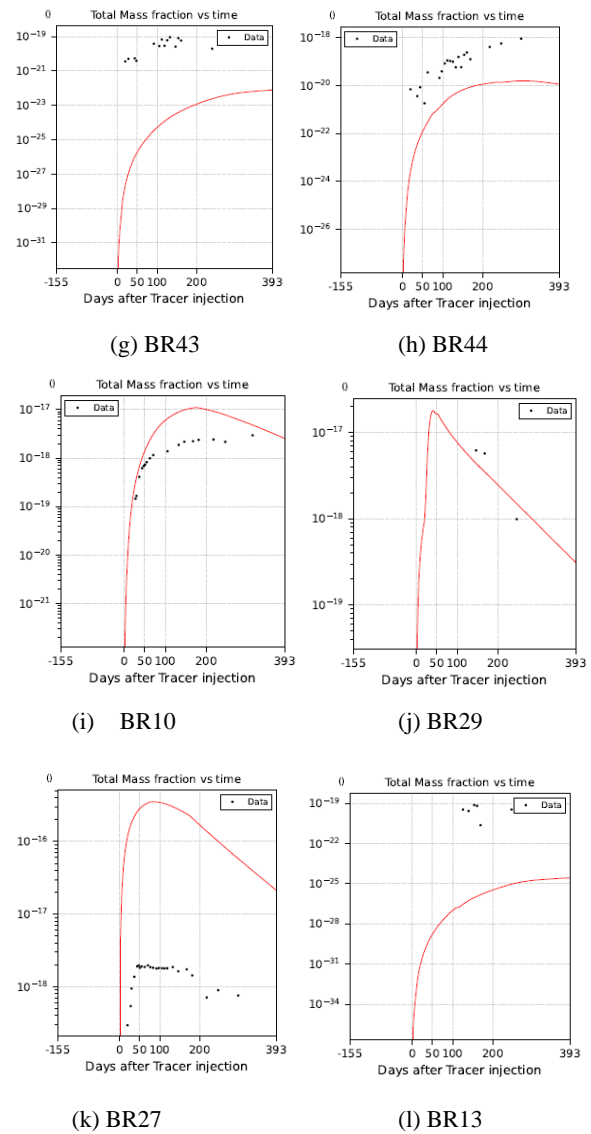
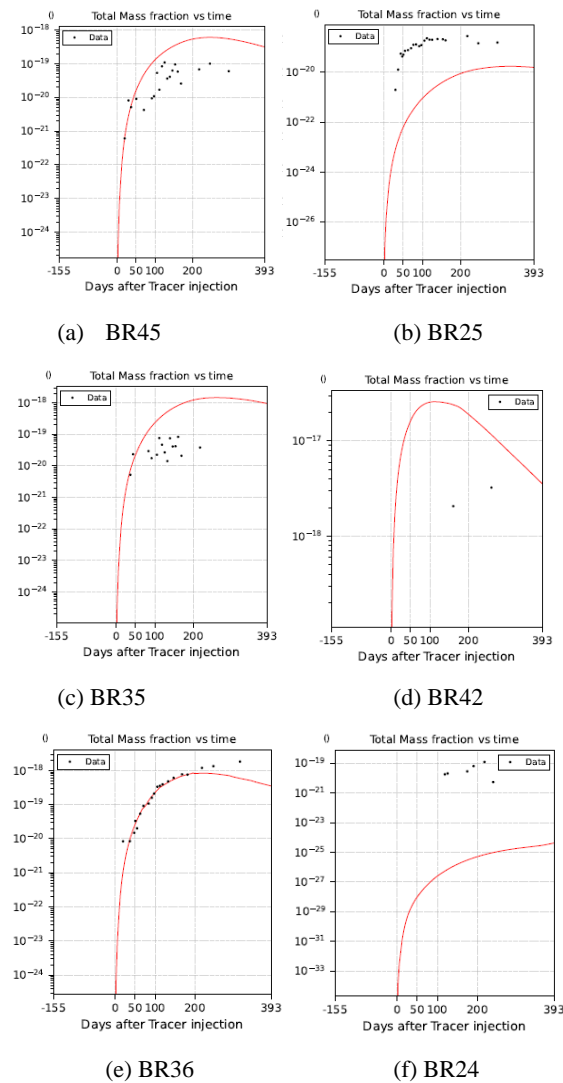


Figure 8. Results for Tracer Test 29. Mass fraction of tracer in the monitor wells BR45, BR25, BR35, BR42, BR36, BR24, BR43, BR44, BR10, BR29 and BR42. Red lines show model results, black dots are data.

Only for BR36 and BR29 is the match of the model to the data reasonable. For the other wells, the model response is either too large or too small, again indicating that some of small-scale permeability distribution in this part of the model is incorrect.

3.4 Modifications to permeabilities

Tracer Test 3

It is a complex task to evaluate the tracer test results in terms of 3D flow paths and the 3D permeability structure. For Test 3, the k_1 and k_2 permeabilities in the area near BR8, BR11 and BR33 on Layer 34 are shown in Figure 9.

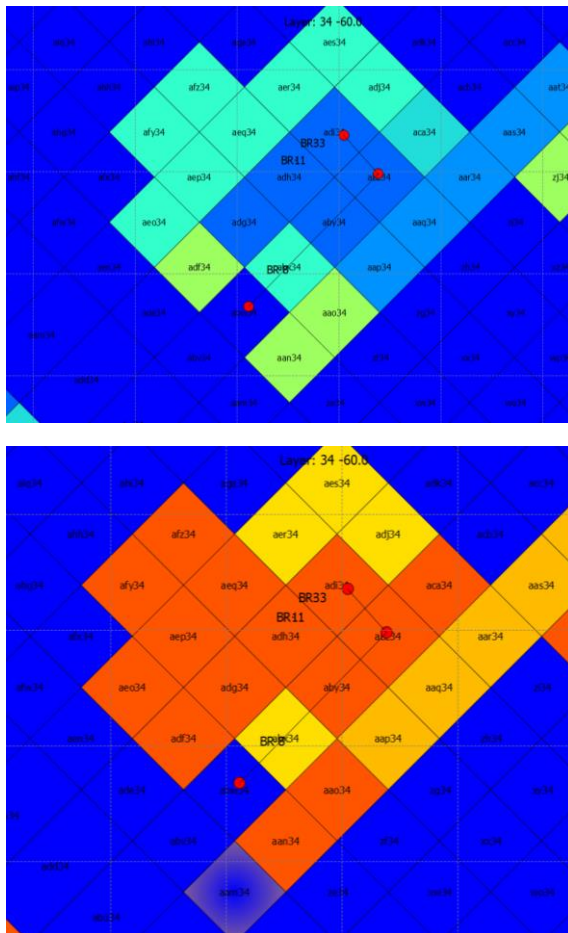


Figure 9: Top - k1 permeability (NE to SW) on Layer 34 (-60 masl, depth ~360 m), Bottom - k2 permeability (NW to SE).

To better match the data the aim is to block the flow from BR33 to BR11 (in the next-door column) while increasing flow in the dog-leg path (with a right-angle bend) from BR33 to BR8 (shown in Figure 9). However, as shown in Table 2, the feedzones for the three wells are at different elevations and the flow fraction for each feed is different and therefore how to best modify the flow paths is a tricky 3D problem.

Table 2: Feedzones for the wells in Tracer Test 3.

Well	Feedzone 1 Elevation masl (feedzone %)	Feedzone 2 Elevation masl (feedzone %)	Feedzone 3 Elevation masl (feedzone %)
BR33	-20 (100%)		
BR11	-180 (41.5%)	-200 (38.5%)	-450 (20%)
BR8	-180 (11.1%)	-275 (11.1%)	-350 (77.8%)

The deep feedzone at -350 masl in BR8 is dominant with an assumed flow fraction of 77.8% whereas the injection in BR33 is shallow at -20 masl indicating that the vertical k3 permeability along the dog-leg track in Figure 9 needs to be increased. The k3 permeability along the dog-leg track is shown in Figure 10. The plot shows there is a patch of low

6

vertical permeability in Layer 44 (-350masl), the main feedzone for BR8. To improve the tracer response in BR8 this patch needs to be made more permeable.

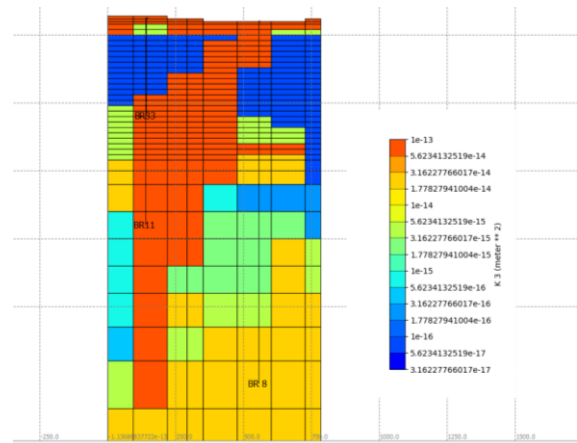


Figure 10: Vertical (k3) permeability along the dog-leg track (shown in Figure 9).

Tracer Test 13

The wells involved in Tracer Test 13 are shown in Figure 11. The model gives a good match to the data in BR23 (see Figure 7) and correctly gives a very small response in BR13. However, the model gives a moderate response in the Layer 47 feed zone of BR22 (the same layer as the top feedzone in BR20), where no response was detected. This suggests that the permeability between BR20 and BR22 in Layer 47 should be reduced.

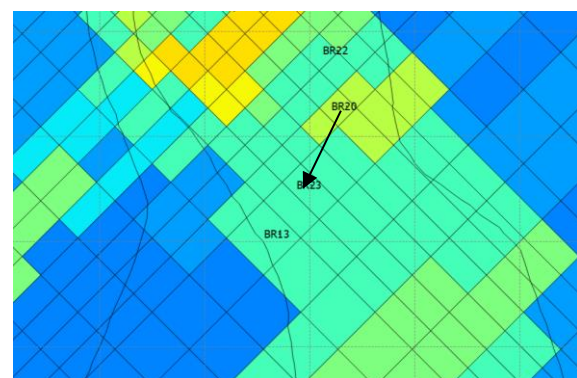


Figure 11: Wells involved in Tracer Test 13 showing an arrow connecting from BR20 to BR23 where there was a response. k2 permeability (NW-SE) on Layer 47 (-650 masl).

Tracer Test 29

The wells involved in Tracer Test 29 are shown in Figure 12. The blue arrows indicate the connection between the injection well, BR7, and wells at which the model response was too low, whereas the red arrows indicate the connection between the injection well, BR7, and wells at which the model response was too high. The connection from BR7 to the two wells where the model gives a good match to the tracer test results are shown by black arrows.

In general, it seems that the k1 permeability (SW-NE) should be decreased and the k2 permeability (NW-SE) should be increased to improve the model result.

The level of discretization in the model is not fine enough to distinguish the responses in nearby wells, e.g., BR25 responds but BR35 and BR45 do not.

In the model there is a good response in both BR36 and BR42 (see Figure 9), but the data shows a weak response in BR42. Based on Figure 12 it is not obvious how to adjust the permeability in the model to achieve this result. It may require a finer grid to arrange a good flow path between BR7 and BR36 that bypasses BR42.

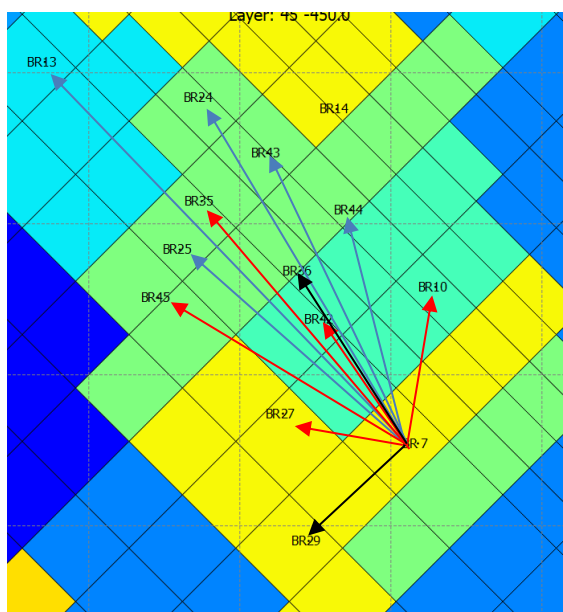


Figure 12: Wells involved in Tracer Test 29. Blue arrows connecting from BR7 to wells where model response was too low, red arrows where model response was too high and black arrows where model response was reasonable. k2 permeability (NW-SE) on Layer 45 (-450 masl).

Again, unravelling the flow paths is a 3D problem as most wells have three feedzones spread from Layer 40 (-180 masl) to Layer 49 (-887.5 masl). The feedzone elevations and flow fractions for each feedzone for BR7, BR36 and BR42 are given in Table 3. Unfortunately, there is nothing obvious in Table 3 that explains a good tracer return at BR36 but a weak return at BR42.

Table 3: Feedzones for the some of the wells in Tracer Test 13.

Well	Feedzone 1 Elevation masl (feedzone %)	Feedzone 2 Elevation masl (feedzone %)	Feedzone 3 Elevation masl (feedzone %)
BR7	-230 (40%)	-450 (40%)	-762.5 (20%)
BR36	-550 (60%)	-887.5 (40%)	
BR42	-350 (47%)	-450 (43%)	-762.5 (10%)

5. CONCLUSION

The results obtained in simulating three tracer tests at Ohaaki using a well-calibrated numerical model are mixed, with most model results showing tracer responses that are either too high or too low. In some cases, it is clear what modifications to the permeability distribution are needed to improve the model results, but in others it is not so clear, and a finer, higher resolution model may be required to obtain better results. So, while tracer tests provide useful information about the permeability distribution in geothermal reservoirs, matching the results of the tracer tests by simulation is more difficult than matching changes in temperature and pressure. The results of the tracer tests depend on finer details of the underground plumbing than are needed to explain temperature and pressure changes.

Nevertheless, simulation of tracer tests is a useful process for improving understanding of the permeability structure of a geothermal reservoir and simulation of some of the other Ohaaki tracer tests will be carried out in the future.

Modifications to the permeability structure of the model suggested by the results of the simulations of the tracer tests will be incorporated into future versions of the model.

ACKNOWLEDGEMENTS

We thank Contact Energy Limited for permission to publish this paper.

REFERENCES

- Bullivant, D.P., McCabe, W.J. & O'Sullivan, M.J.: Ohaaki tracer testing prior to December 1989 - A summary of the tests conducted by the Institute of Nuclear Sciences. Technical report, Department of Engineering Science, University of Auckland (1990).
- Clotworthy, A.W.: Selection and testing of reinjection wells for the Ohaaki geothermal field. *Proc. 11th New Zealand Geothermal Workshop* (1989).
- Croucher, A., O'Sullivan, M., O'Sullivan, J., Yeh, A., Burnell, J., Kissling, W.: Waiwera: A parallel open-source geothermal flow simulator. *Computers and Geosciences*, 141 (2020).
- Croucher, A., O'Sullivan, M.J. & O'Sullivan, J.P.: Modelling tracers using the Waiwera geothermal flow simulator. *Proc. 43rd New Zealand Geothermal Workshop*. Wellington (2021).
- Gómez-Díaz, E., S. Scott, S., Ratouis, T., & Newson, J.: Numerical modeling of reinjection and tracer transport in a shallow aquifer, Nesjavellir Geothermal System, Iceland. *Geothermal Energy*, 10(1), (2022).
- Grant, M.A.: Summary of tracer and interference testing at Ohaaki – revised Dec 2011 (PFB). Report from MAGAK, Quantitative Decisions (2011).
- McCabe, W.J.: BR16, BR29, BR39 & BR40 tracer tests Ohaaki - February 1990. Report INS-R-423, Institute of Nuclear Sciences (1990).

- McCabe, W.J.: BR12 reinjection tracer test September 1990. Report DSIRPS-C-17, DSIR (1991).
- McCabe, W.J.: BR40 reinjection tracer test Ohaaki March 1992. Report DSIRPS-C-80, DSIR (1992a)
- McCabe, W.J.: BR7 reinjection tracer test Ohaaki - June 1991. Report DSIRPS-C-71, DSIR (1992b).
- McCabe, W.J.: BR16 tracer test Ohaaki, August 1992. Report 633 890 40, IGNS (1993).
- McCabe, W.J.: BR30 tracer test Ohaaki, July 1993. Report 63440C 30, IGNS (1994).
- McCabe, W.J.: BR11 tracer test Ohaaki, June 1994. Report 63440C 30A, IGNS (1995a).
- McCabe, W.J.: BR38 tracer test Ohaaki, February 1994. Report 63440C 30B, IGNS (1995b).
- McCabe, W.J.: BR41 tracer test Ohaaki, November 1994. Report 63440C 30C, IGNS (1995c).
- McCabe, W.J., Clotworthy, A.W., & Morris, C.: Results of repeat tracer testing at Ohaaki, New Zealand. *Proc 17th NZ Geothermal Workshop* (1995).
- O'Sullivan, J.P., Popineau, J., Gravatt, M., Renaud, T., Riffault, J., Croucher, A., Yeh, A. & O'Sullivan M.J.: An integrated, mesh-independent geothermal modelling framework. *Environmental Modelling and Software*, 163, 105666 (2023a).
- O'Sullivan, J.P., Gravatt, M., Renaud, T., Riffault, J., & O'Sullivan M.J.: Update of the numerical model of the Ohaaki Geothermal Field 2021-23. Report OH2023_01, (for Contact Energy Limited) Geothermal Institute, University of Auckland (2023b)
- Popineau, J., O'Sullivan, J. P., O'Sullivan, M. J., Archer, R., & Williams, B.: An integrated Leapfrog/TOUGH2 workflow for a geothermal production modelling. *Proc. 7th African Rift Geothermal Conference* (ARGeo). Kigali, Rwanda. (2018).
- Renaud, T., Popineau, J., Riffault, J., O'Sullivan, J., Gravatt, M., Dekkers, K., Yeh, A., Croucher, A., O'Sullivan, M.: Practical workflow for training in geothermal reservoir modeling. *Proc. 43rd New Zealand Geothermal Workshop*, Wellington, New Zealand. (2021).
- Yeh, A., Croucher, A.E., O'Sullivan, M.J.: Recent developments in the AUTOUGH2 simulator. *Proc. TOUGH Symposium 2012*, Berkeley, California, USA (2012).

APPENDIX. DETAILS OF THE THREE TRACER TESTS

Test	Test 3	Test 13	Test 29
Injection well	BR33	BR20	BR7
Date	21/5/1977	17/10/1985	6/6/1991
Tracer	¹³¹ I	¹³¹ I	¹²⁵ I
Amount	7.3 Ci (270 GBq)	1.9 Ci (70 GBq)	0.524 Ci
Observation wells	BR8, BR11	BR13, BR22, BR23	BR10, BR13, BR14, BR24, BR25, BR27, BR29, BR35, BR36, BR42, BR43, BR44, BR45
Response wells	BR8, BR11	BR23	BR10, BR25, BR27, BR29, BR36, BR42, BR44
No, or very low response wells		BR13, BR22	BR13, BR14, BR24, BR35, BR43, BR45
Injection rate	80 kg/s	35 kg/s	220 t/h
References	Grant (2011), Bullivant et al. (1990)	Grant (2011), Bullivant et al. (1990)	Grant (2011), McCabe (1992b)